Seismic Response Analysis of Gravity Retaining Walls

Mohamed Husain and Othman Shaalan

Structural Engineering Department, Faculty of Engineering, Zagazig University, mo_husain2000@yahoo.com

Abstract: The nonlinear inelastic seismic response analysis is performed using finite element model, with both material and geometrical nonlinearity. The purpose of the current study is to determine effects of the soil-structure interaction on the retaining wall seismic response. Two-dimensional plain strain finite element analytical model is developed for concrete gravity retaining walls founded on and retaining dry sand. The commercial software package ADINA is employed in the study. The soil and wall are modeled using four-node plane strain element with two displacement degrees of freedom at each node. The nonlinear response of soil is represented by Mohr-Coulomb model, and the inelastic behavior of the concrete is modeled by the available concrete element in ADINA. The soil-structure interaction is simulated with the contact surface approach. Free vibration analysis was performed to obtain the system modal parameters, and parametric seismic response analyses are conducted on several soil-wall models. The study results show that the soil type, retaining wall geometry as well as earthquake intensity have significant effects on the wall response.

[Mohamed Husain and Othman Shaalan. **Seismic Response Analysis of Gravity Retaining Walls.** *J Am Sci* 2012;8(12):599-607]. (ISSN: 1545-1003). http://www.jofamericanscience.org. 83

Keyword: Seismic response, finite element, nonlinear, inelastic, retaining wall, earth pressure.

1. Introduction

Gravity retaining wall that supports dry cohesionless backfills is considered one of a major group of the earth-retaining structures. These structures are damaged during strong earthquakes due to seismically induced lateral earth pressure and inertial effects on the wall itself. Dynamic response analyses of retaining walls are classified in three groups: 1- Limit state methods (Mononobe-Okabe, or O-M method) [1-5], where the wall is sufficiently displaced at its base to mobilize the backfill full shearing strength. 2- Elastic methods, in which wall is considered fixed against both deflection and rotation at the base, and backfill is presumed to respond as a linearly elastic or visco-elastic material [6-8]. 3- Inelastic (plastic) nonlinear finite element methods, that assumes nonlinear behavior of the wall and the retained soils. The first two methods yield widely different results, where wall horizontal pressure and associated forces computed by elastic analysis are generally 2 to 3 times larger than those determined by limit state methods [9-14].

The dynamic response problem of retaining walls has been attracted researchers for decades. Seed and Whitman [4] have conducted wall analysis combines wave propagation in a visco-elastic continuum with lumped plastic deformation model. Richard and Elms [8] studied the seismic behavior of gravity retaining wall by adding the horizontal and vertical inertia terms to the Mononobe – Okabe’s analysis to suggest a new seismic design approach for gravity retaining wall. Matsuo and Ohara [5] have used the elastic wave equation to estimate a solution for dynamic lateral earth pressure against vertical solid quay walls during earthquakes. Scott [6] has devised a simple model for experimentally evaluating the dynamic soil pressures induced by ground shaking on walls retaining an elastic stratum. Wood [7] has proposed an idealized non-yielding rigid wall model assuming plane strain, homogeneous and isotropic soil and rigid element resting on rock. He concluded that the dynamic force resultant on the wall acts approximately at 0.6 H from the base.

Nadim and Whitman [9] proposed a two-dimensional plane-strain finite element model that is capable of computing permanent displacements taking in to account the amplification of ground motion in the backfill. They found that earthquake loading causes stress redistribution following an earthquake with residual force on the wall about 30% greater than the static active force. Zhao and Valliappan [10] developed a simple method for dynamic analysis of reinforced retaining walls during earthquakes based on the plane strain assumption, finite and infinite element and the concept of the equivalent material behind the wall. They have concluded that retaining wall configurations has a significant effect on the amplification factor of the structure. Li [13] extends the Veletsos and Younan’s approach to include foundation flexibility and damping in the analysis of rigid retaining wall. AL-Homoud and Whitman [14] developed a two-dimensional finite element analytical model to analyze the seismic response of rigid high way bridge retaining abutments.

Choudhury and Chatterjee [15] developed an extension of the Veletsos and Younan study [11,12], they used a mass-spring-dashpot dynamic model with two degrees of freedom to arrive at the total active earth pressure under earthquake time history loading. They also presented non dimensional design charts for rapid calculation of active earth pressures. Choudhury and Subba-Rao [16, 17] in two different studies, obtained an estimate for the seismic passive earth pressure against retaining walls by using logarithmic spiral, and composite curve failure surface assumptions and a pseudo-static method. Recently, Linda and Sitar [18] have performed experimental and analytical program to evaluate the magnitude and distribution of seismically induced lateral earth pressures on cantilever retaining walls with dry medium dense sand backfill. Results from two sets of dynamic centrifuge experiments and two-dimensional nonlinear finite-element analyses show that maximum dynamic earth pressures monotonically increase with depth. Moreover, dynamic earth pressures and inertia forces do not act simultaneously on the cantilever retaining walls. Furthermore, seismic earth pressures on cantilever retaining walls can be neglected at accelerations below 0.4 g. Giarlelis and Mylonakis [19] have examined the dynamic response of rigid and flexible walls retaining dry cohesionless soil in light of experimental results and analytical elasto-dynamic and limit analysis solutions. Experimental findings from three different testing programs on retaining walls are presented and compared with theoretical predictions. They have shown that wall flexibility, which is not taken into account in classical design should be considered to establish the point of application of seismic thrust on the wall.

Many gravity-type retaining walls have failed during strong earthquakes, while flexible reinforced concrete walls have performed well and have experienced limited damage, as has been documented in post-earthquake reconnaissance reports. In the 1995 Mw 7 Kobe earthquake a wide variety of retaining structure were subject to peak ground accelerations (PGA) as high as *0.80 g*. Masonry and unreinforced concrete gravity walls were heavily damaged, while L-shape reinforced concrete flexible walls sustained limited damage. In the 1994 Mw 6.8 Northridge

earthquake temporary anchored walls were subjected to PGA level between of *0.20 g* and *0.60 g*. Measured deflections of walls were less 1 cm and there was no visual change attributable to seismic shaking. In the 1999 Ms 5.9 Athens (Parnitha) earthquake several metro-stations were subjected to nearly *0.50 g* PGA, no damage was visible after the earthquake [20-22].

The purpose of this paper is present the modeling and analysis of the inelastic nonlinear seismic response of gravity concrete walls. Also to determine effects of the soil-structure interaction on the retaining wall seismic response, and to obtain reasonably accurate seismic design forces for gravity retaining walls. Two-dimensional plain strain finite element model(FEM) is developed for a concrete gravity retaining wall founded on and retaining dry sand. Free vibration analysis and parametric seismic response analyses are conducted on several soil-wall models. The commercial software package ADINA is used for the numerical analyses.

Finite Element Analysis

ADINA "Automatic Dynamic Incremental Nonlinear Analysis" is a computer program developed based on finite element theory. Two-dimensional solid element is one of the elements available in ADINA program [23]. For the plane stress, plane strain, generalized plane strain, index symmetric the elements must be defined in the YZ plane, in which Y represents the horizontal axis and Z represents the vertical axis, As shown in Figure (1). The ADINA elements are usually isoperimetric displacement-based finite elements which basic assumptions are:

The coordinates are:

$$y = \sum_{i=1}^{q} h_i y_i \qquad z = \sum_{i=1}^{q} h_i z_i \qquad (1)$$

For the displacements in plane stress, plane strain, and axisymmetric elements, and coefficient between the surfaces.

$$v = \sum_{i=1}^{q} h_i v_i \qquad w = \sum_{i=1}^{q} h_i w_i \qquad (2)$$

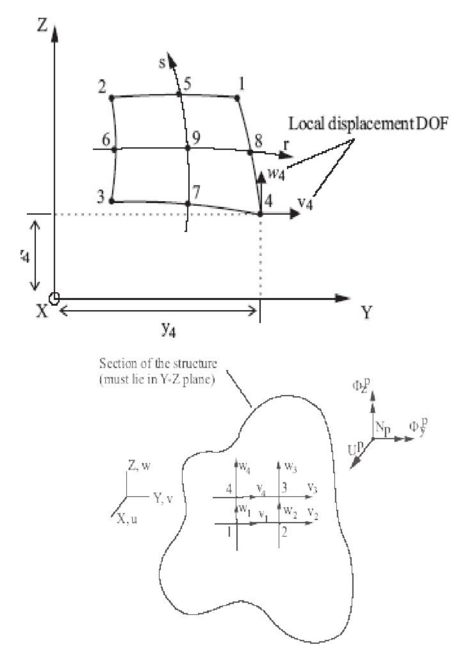

Figure (1) The Nodal Coordinates and Displacements of the 2-D Solid Elements

The displacements in generalized plane strain elements:

$$u = xU^{p} - x(y - y^{p})\Phi_z^{p} + x(z - z_p)\Phi_y^{p}$$

$$v = \sum_{i=1}^{q} h_i v_i + \frac{1}{2}x^2\Phi_z^{p} \qquad (3)$$

$$w = \sum_{i=1}^{q} h_i w_i - \frac{1}{2}x^2\Phi_z^{p}$$

Where:

$h_i(r,s)$ = interpolation function corresponding to node *i;*

(r,s) = isoperimetric coordinates;

q = number of element nodes excluding auxiliary node in generalized plane strain;

$y_b z_i$ = nodal point coordinates;

$v_b w_i$ = nodal point displacements;

$U^{p}, \Phi_y^{p}, \Phi_z^{p}$ = degrees of freedom of the auxiliary node; and

x_p, y_p, z_p = coordinates of the auxiliary node;

In ADINA computer program the calculations of all element matrices and vectors are performed with numerical Gauss integration from 2×2 to 6×6. Note that in geometrically nonlinear analysis, the spatial positions of the Gauss integration points change continuously as the element undergoes deformations, but throughout the response, the same material particles are at the integration points.

The concrete element is from the material models available in ADINA. The element can be used with small displacement and large displacement formulations. The basic material characteristics are: Tensile failure at maximum, relatively small principal tensile stress and compression crushing failure at high compression. Strain softening from compression crushing failure to an ultimate strain, at which the material totally fails.

There are many types of geotechnical material model available in ADINA: Curve description, Drucker-Prager, Cam-Clay and Mohr-Coulomb material model. The Mohr-Coulomb model is used to model the soil behind and under the wall.

One of the soil-structure interaction problems is the local nonlinear behavior of the interface between the soil and the structure. There are two main approaches to model the interface problem; namely contact element and contact surface approaches. Contact surface approach is used in the current research. In this approach, the nodes of the two surfaces are defined relative to each other by friction

One of the contact-surface modeling procedures available in ADINA, is the master-slave technique, where the model is divided into master and slave sub-models. The two sub-models interact along a user-defined contact surface. using the sub-structural approach, the program determines the displacement for the master nodes on the contact surface, then the slave nodes [23].

There are two classes of boundary conditions: essential boundary conditions, such as prescribed displacement (and rotation) boundary conditions, and natural boundary conditions, such as applied force and moment boundary conditions. In this study the two sides of the model are modeled using a displacement equal to zero in the horizontal direction and free in the vertical direction, during the static mode, to enable the soil to consolidate under static loads. In the dynamic mode, under earthquake load, the mechanism of repeatable side boundaries was used.

The general form of the finite element system equilibrium equations is that multiplying the stiffness matrix by the displacement vector will lead to the force vector, as follows:

$$KU = R \qquad (4)$$

ADINA solves this set of equations using a direct solution scheme or an iterative solution scheme as a linear Static Analysis – Solution. In nonlinear static analysis the equilibrium equations to be solved are:

In the nonlinear static analysis, the equilibrium equations to be solved are:

$$^{t+\Delta t}R - {}^{t+\Delta t}F = 0 \qquad (5)$$

Where; $^{t+\Delta t}R$: is the vector of externally applied nodal loads at time step t+Δt, and $^{t+\Delta t}F$: is the force vector equivalent to the element stresses at time step t+Δt.

The nonlinearity may come from the material properties, the kinematics assumptions and the use of contact surfaces. The solution of the finite element equations is usually obtained by direct integration procedures. The incremental finite element equilibrium equations used in implicit time integration (without equilibrium iterations) are represented by the following formula:

$$\mathbf{M}\,{}^{t+\Delta t}\ddot{\mathbf{U}} + \mathbf{C}\,{}^{t+\Delta t}\dot{\mathbf{U}} + {}^{t}\mathbf{K}\,\mathbf{U} = {}^{t+\Delta t}\mathbf{R} - {}^{t}\mathbf{F} \qquad (6)$$

Where; M is the mass matrix, C is the damping matrix, K is the system stiffness matrix, R is the externally applied load vector at time t+Δt, and F is the consistent nodal force vector due to the incremental displacement vector, $^{t+\Delta t}U$.

Table (1) illustrates the different parameters of chosen soil types. However, in computer program

ADINA, it was a problem to insert zero values for Cohesion parameters in the model so the values of cohesion must be modified to avoid the over-flow errors.

Table (1):The different parameters of cohesionless soil types

Soil type	Density ρ Kg/m^3	Cohesion C	Friction angle ϕ	Elastic modulus E (Mpa)	Angle of Dilation φ
Loose sand	1600	0	31	20	1
Medium dense sand	1800	0	36	100	6
Dense sand	1900	0	41	200	11

The Northridge earthquake excitation record is used in the current dynamic response analysis, Figures (2 and 3) show its displacement and acceleration time-history record.

Figure (4) shows the typical section of the retaining wall-soil model and its dimensions. Seventy meters to the left, right and soil below the wall is included. Figure (5) shows the finite element meshing of the proposed wall-soil system model into finite element.

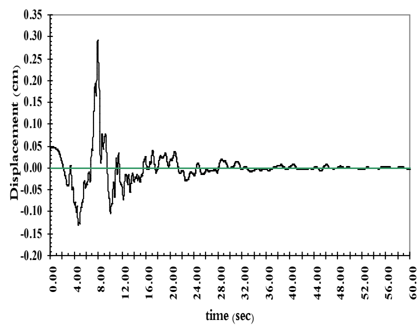

Figure (2) Displacement Time-History of the Northridge Earthquake

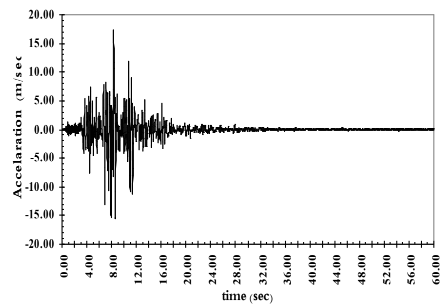

Figure (3) Acceleration Time-History of the Northridge Earthquake

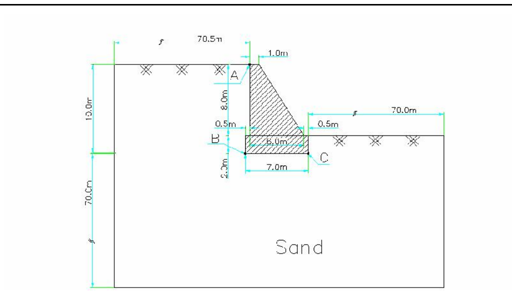

Figure (4) : Typical section of proposed model

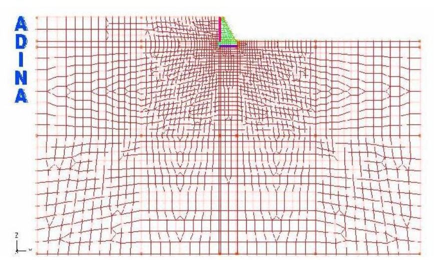

Figure (5) Finite element discretization of the proposed model

3. Results and Discussions

Free Vibration Analysis

At first the free vibration analysis of the wall-soil system is carried out, in order to obtain the significant modes of vibrations and their frequencies or the system natural periods of vibrations. The mode shapes and the natural period of vibrations give clear description of the model dynamic characteristics which impact the seismic response calculations. They always needed for any pseudo-dynamic response algorithm (response spectrum method). The natural period of vibration of the wall-soil system versus B/H (wall width/wall height) ratio is drawn in Figures (6-8). The first and second modes values are very flexible (period of vibrations larger than 4 sec.), and therefore they have no significant effect on the retaining wall response because earthquake of period larger than 3.0 sec. are extremely rare. The numerical analysis for the first (fundamental) and second periods were unstable, and cannot be drawn versus the B/H ratio.

Figures (6-8) show the natural period of motion versus B/H ratio for the third, fourth and fifth mode of vibrations, respectively. The general observation on these figures is that the natural period of vibration for dense sand is smaller than that of the medium- dense sand, which in turn is smaller than that of the loose sand. These results match the elastic response spectrum curve of Figure (9). Another important observation on figures is that the gravity wall geometry (B/H) has insignificant influence on the natural period of the wall-soil system.

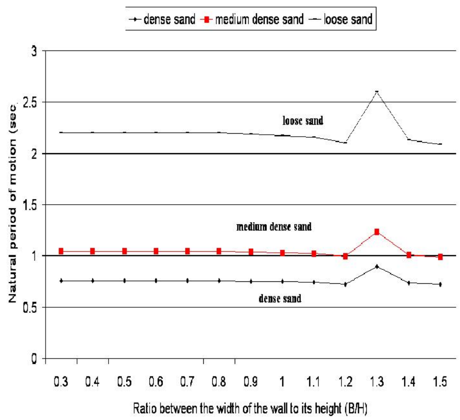

Figure (6): Natural period versus B/H ratio for the third mode

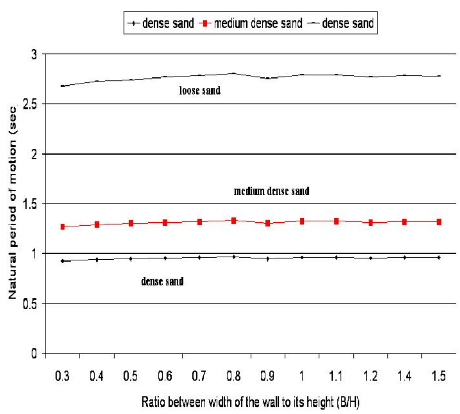

Figure (7): Natural period versus B/H ratio for the fourth mode

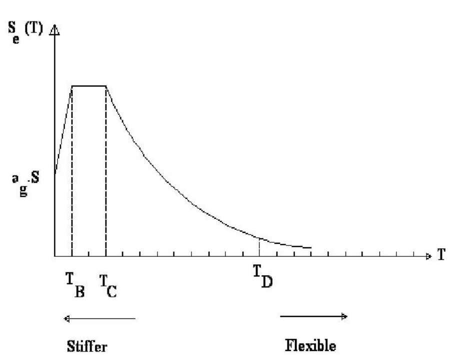

Figure (8): Natural Period versus B/H ratio for the fifth mode

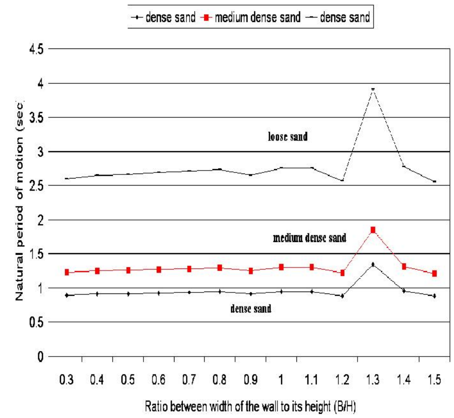

Figure (9): Elastic horizontal response spectrum curve

Seismic Response Analysis

The seismic response of gravity wall-soil system is studied for various types of cohesion soils, namely loose sand, medium dense sand and dense sand, and with different earthquake intensity.

Figure (10) shows the time history of the wall horizontal translation (displacement at point B) due to Northridge earthquake for loose sand, medium dense sand and dense sand backfills. Figure (11) shows the time history of the wall vertical displacement (at point B) due to Northridge earthquake for loose sand, medium dense sand and dense sand. It is observed that the wall translation is smaller for more densely soils. It is also observed that the relative vertical displacement is generally small (about one tenth of the horizontal one). From the above, it is concluded that the soil have two significant interaction effects on earthquake excitations. Firstly, the mass of soil (or the degree of compaction) affects the wave propagation velocity. Secondly, the damping nature of soil which acts as an energy absorption for seismic waves.

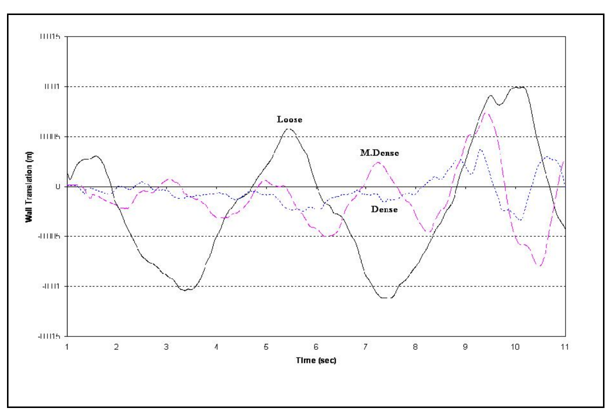

Figure (10): Time history of the wall horizontal translation for loose, medium-dense and dense sand

Figure (12) shows the values of static earth pressure distribution along the wall height of the retaining wall for loose, medium dense and dense sand. It is observed that the static earth pressure decreases for more densely sand although dense sand has larger density. That is due to modulus of active earth pressure which decreases as the friction angle increases. Figure (13) shows the ratio between maximum values of static plus dynamic earth pressure /static earth pressure on the retaining wall due to an Northridge earthquake for loose, medium dense and dense sand. It can be observed that, unlike static earth pressure, the dynamic earth pressure on the wall increases as the soil density increases. That is may be due to the amplification of soil motion which increases for more densely sand. Also, it may be due to the movement of wall which is larger for loose sand than for dense one. That is confirm Zhao and Valliappan conclusion which reported that the backfill soil behind the retaining wall has considerable effects on the response of the retaining walls during higher frequency seismic excitations. From Figure (13) one may conclude that earthquake converts the triangular distribution of the earth pressure for case of dense sand into uniform distribution.

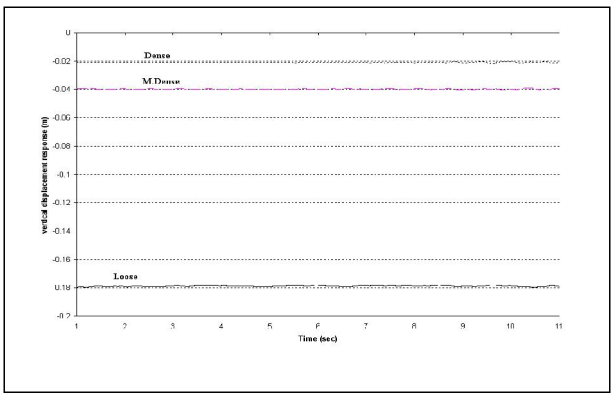

Figure (11): Time history of vertical displacement for loose, medium-dense and dense sand soil

Figure (14) shows the amplification factor of earth pressure exerted on the wall for various types of soil. It is observed that change in values of the earth pressure is more substantial in the case of denser sand. Denser backfill soils produce higher earth pressure than looser backfill soils. This coincide with the Zhao and Valliappan's conclusion. Figure (15) shows the amplification factor of over-turning bending moment exerted on the retaining wall for various types of backfill soils. It was observed that change in values of the wall over-turning moment is more substantial in case of denser sand under dynamic loads. Wall over-turning moment values of denser backfills are higher than that of less denser ones.

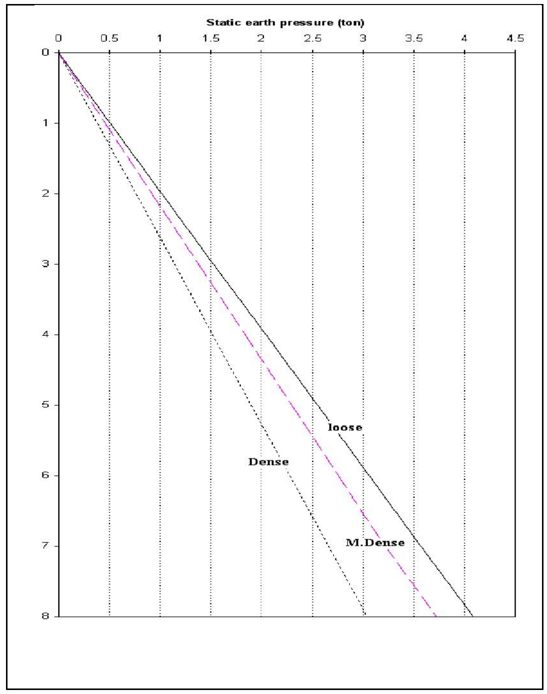

Figure (12): Values of static earth pressure on wall for loose, medium dense and dense sand

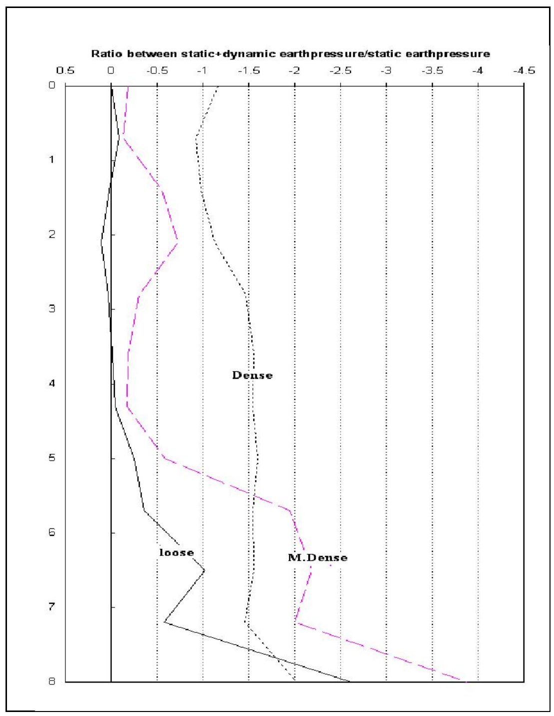

Figure (13): Peak (static + dynamic)/static earth pressure on wall for loose, medium dense and dense sand

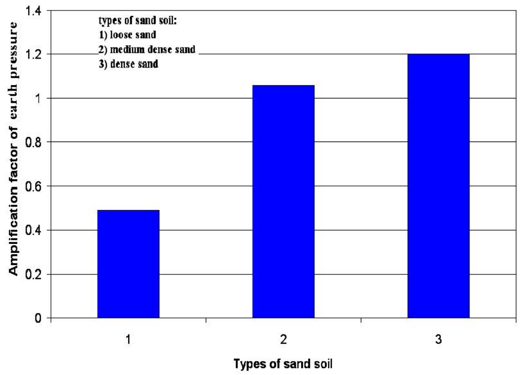

Figure (14): Amplification factor of earth pressure exerted on the wall stem for various types of sands

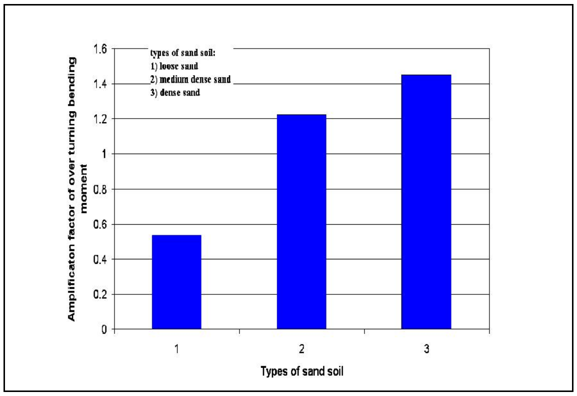

Figure (15) shows the amplification factor of over-turning bending moment exerted on the retaining wall for various types of backfill soils.

The effect of changing the wall width on its behavior under the earthquake excitation is subsequently studied. Figure (16) shows the time history of the horizontal displacement response at point B due to Northridge earthquake for different wall widths: 8.0 m, 6.0 m, 5.0 m and 4.0 m. One may observe that there is no much difference between the values of horizontal displacement at point B for the four cases of wall widths. Figure (17) shows the time history of the wall vertical translation due to Northridge earthquake for the four cases of wall widths. The wall vertical translation is vertical displacement at point B. It is observed that the vertical displacement decrease with decrease of wall width. Finally, Figure (18) shows the time history of the wall rotation due to Northridge earthquake for the different wall width cases. It can be observed that the wall rotation decreases as the wall width increases. Therefore, increasing the wall width does not affect wall horizontal translation but has a significant effect on both vertical displacement and wall rotation.

Decreasing the wall width increase its flexibility, and when the wall becomes more flexible, its vertical displacement response decreases. Also, the wall rotation decrease for more flexible walls and confirm AL-Hamoud and Whitman conclusions. From previous figures, it was concluded that the inertia of the wall has a significant effect on its dynamic response.

Figure (19) shows the distribution of the dynamic earth pressure on the wall/static earth pressure due to Northridge earthquake for different widths, 8.0 m, 6.0 m, 5.0 m and 4.0 m. Figure (19) shows that when the wall width decreases, the wall earth pressure decreases. That is due to the flexibility of the wall which increases with decreasing the wall width. Also when the wall width increases, the wall rigidity increases which increases the earth pressure, consequently the base shear and over turning bending moment on the wall decreases. That is confirming Veletsos and Younan conclusions as they reported that both the magnitudes and distributions of the wall earth pressure and associated forces induced by horizontal ground shaking are quite sensitive to flexibilities of the wall and its base. Increasing the flexibility reduces the horizontal extensional stiffness of the retained medium relative to its shearing stiffness and this reduction decreases the proportion of the soil inertia forces that gets transferred to the wall and hence the forces develop.

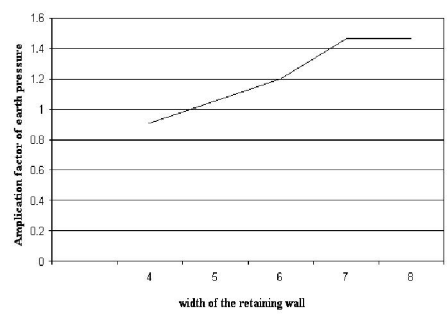

Figure (16): Time history of wall horizontal displacement for different widths

Figure (20) shows the amplification factor of the earth pressure versus wall width and figure (21) shows the amplification factor of over-turning moment versus wall width. It is observed from the Figures (20 and 21) that increasing the wall width amplify the wall seismic responses. It is also noticed that the amplification factor of the earth pressure and over-turning bending moment is varied from 1.1 for flexible wall to 1.8 for more rigid wall.

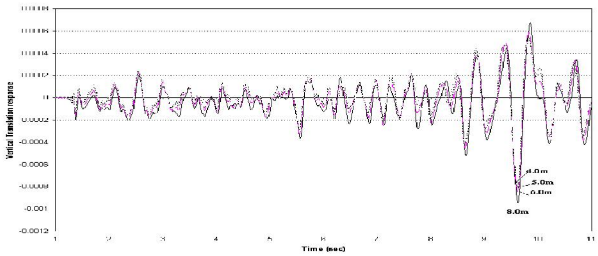

Figure (17): Time history of wall vertical displacement for different widths

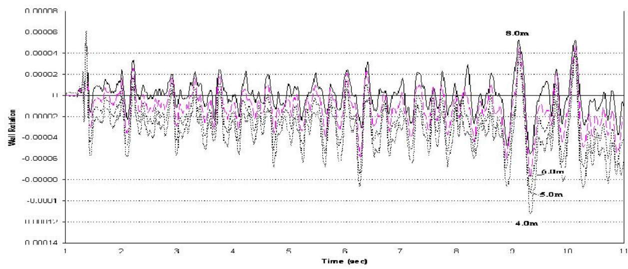

Figure (18): Time history of wall vertical displacement for different widths

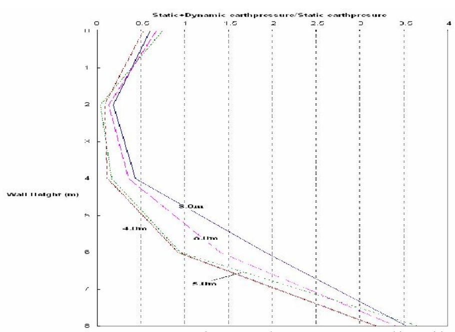

Figures (19): Dynamic earth pressure distribution on wall of different widths

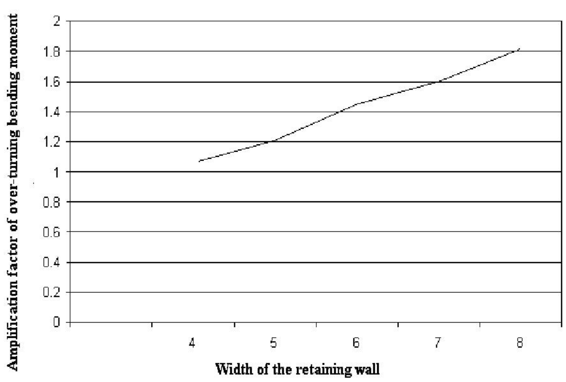

Figure (20) shows the amplification factor of the earth pressure versus wall width and figure

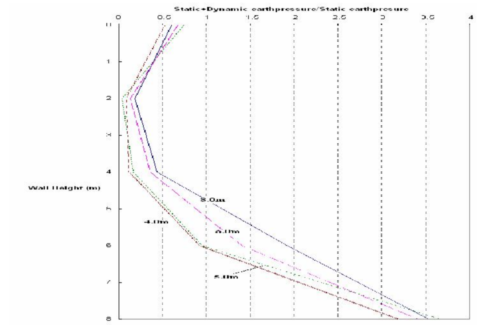

Figure (21): Amplification factor

In order to examine the effect of the earthquake intensity on the retaining wall response, it is suggested to multiply the Northridge displacement values × 2 and divide it by 2 to study the effect of stronger and weaker earthquake intensity on the wall response.

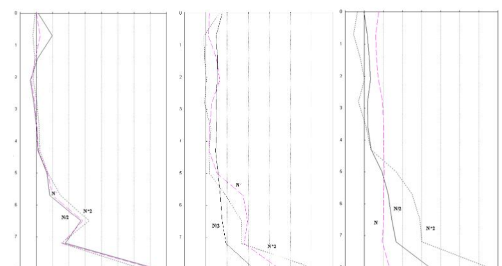

Figure (22): Seismic /static earth pressure on the wall for case of loose, medium - dense and dense sand backfills, respectively

Figure (22) shows the ratio between the Seismic dynamic earth pressure/static earth pressure along the wall stem at weaker and stronger earthquake intensity for cases of loose, medium-dense and dense backfills, respectively. From Figure (22) one may observe that the seismic dynamic earth pressure decreases when the earthquake intensity increases. Therefore a stronger earthquake might cause a reduction of the total force on the wall if at rest static conditions exist before the ground shaking.

Conclusions:

From the previous analysis and discussions on seismic response of gravity retaining wall constructed in dry sand, the main conclusion are summarized as follow:

1- From free vibration analysis, it is found that the wall geometry has insignificant effect on the natural period and mode shape of the wall-soil system.
2- Natural period of vibration longer for loose sand backfills, and shorter for dense sand backfills.
3- The denser backfills may exert larger dynamic earth pressure on the wall than looser backfills. Consequently, dense sand give larger base shear

and over-turning moment than loose sand. Although the looser soil exerts larger static earth pressure than dese sand.

4- Values of horizontal and vertical displacement of the wall during earthquake decrease as backfill compaction increase.

5- The vertical displacement of the wall is about tenth of the horizontal translation.

6- As the wall width increases, the seismic dynamic earth pressure increases and the base shear and over turning moment increases.

7- Earthquake intensity affects the seismic earthquake response, where a high intensity earthquake might cause a reduction of the total force on the wall.

Corresponding author

References

1 Mononobe, N., "Earthquake-proof Construction of Masonry Dams," Proceedings, World Engineering Conference, 9, 1929.
2 Mononobe, N., and Matsue, H., "On the Determination of Earth Pressures during Earthquakes, "Proceedings, World Engineering Conference, V. 9, 1929.
3 Okab, S., "General Theory of Earth Pressure," Journal of Japanese society of Civil Engineers, Tokyo , Japan, 12, (1): 1926.
4 Seed, H. B., and Whitman, R. V., " Design of Earth Retaining Structures for Dynamic Loads, " presented at the June, 22-24, 1970 ASCE Specially Conference – Lateral Stresses in the Ground and Design of Earth Retaining Structures, held at Cornell University, Ithaca, N.Y.
5 Matsuo, H., and Ohara, S. (1960) "Lateral Earth Pressure and Stability of Quay walls during Earthquakes." Proc., 2nd World Conference Earthquake Engineering, International Association for Earthquake Engineering, Tokyo, Japan.
6 Scott, R. F. (1973). "Earthquake-induced pressures on retaining walls." Proc. 5th World Conf. on Earthquake Engineering., International Association of earthquake Engineering, Tokyo, Japan, 2, 1611-1620.
7 Wood, J. H. "Earthquake-induced pressures on retaining walls. " Rep. EERL 73-05 , Earthquake Engineering Res. Lab., California Institute of Technology, Pasadena, CA, USA, 1973.
8 Richards, R. J., and Elms, D., "Seismic Behavior of Gravity Retaining Walls" Journal of the Geotechnical Engineering Division, ASCE, 105, (GT4): 1979: 449-464.
9 Nadim, F., and Whitman, R.V. "Seismically Induced Movement of Retaining Walls." J. Geotechnical Engineering., ASCE, 109 (7): 915-931, 1983.
10 Zhao, C. and Valliappan, S., " Dynamic Analysis Of A Reinforced Retaining Wall Using Finite And Infinite Elements Coupled Method ,"Journal Of Computers And Structures, 47, (2), : 239-244, 1993.
11 Veletsos A. S., and Younan A. H., "Dynamic Response of Cantilever Retaining Walls", Journal of Geotechnical and Geoenvironmental Engineering ,ASCE, 1997, 123 : 161-172.
12 Veletsos AS, Younan AH, "Dynamic Modeling and Response Of Soil-Wall Systems," Journal of Geotechnical Engineering, ASCE, 120, (12): 1994: 2155-2179.
13 Li. X., "Dynamic Analysis Of Rigid Walls Considering Flexible Foundation," Journal of Geotechnical and Geoenvironmental Engineering, ASCE, 125, (9) 1999: 803-807.
14 AL-Homoud A. S. and R. V. Whitman, "Seismic Analysis And Design Of Rigid Bridge Abutments Considering Rotation And Sliding Incorporating Non-linear Soil Behavior," Journal of Soil Dynamic and Earthquake Engineering, 18, January 1999: 247-277.
15 Choudhury, D. and Chatterjee, S., "Dynamic active earth pressure on retaining structures", Sadhana, Academy Proceedings in Engineering Sciences, 31(6),pp. 721-730 (2006).
16 Choudhury, D. and Subba-Rao, K.S., "Seismic passive resistance in soils for negative wall friction", Canadian Geotechnical Journal, 39(4), pp. 971-981 (2002).
17 Subba-Rao, K.S. and Choudhury, D., "Seismic passive earth pressures in soils", Journal of Geotechnical and Geoenvironmental Engineering, ASCE, 131(1), pp.131-135 (2005).
18 Linda A. A., and Sitar, N., "Seismic Earth Pressures on Cantilever Retaining Structures", ASCE, Journal of Geotechnical and Geoenvironmental Engineering, Vol. 136, No. 10, October 2010, pp. 1324-1333.
19 Giarlelis, C., and Mylonakis, G., "Interpretation of dynamic retaining wall model tests in light of elastic and plastic solutions", Journal of Soil Dynamics and Earthquake Engineering, Vol. 31, Issue 1, January 2011, pp. 16-24.
20 Russell A. Green, C., Guney-Olgun, Robert M. Ebeling and Wanda I. Cameron, " Seismically Induced lateral Earth Pressure on a Cantilever Retaining Wall", Proceeding of The Sixth US Conference and Workshop on Life Earthquake engineering (TCLEE2003), ASCE, August 10-13, 2003, long beach, CA.
21 Gazetas, G., Psarropoulos, P. N., Anastasopoulos, I., and Gerolymos, N., "Seismic behavior of flexible retaining systems subjected to short-duration moderately strong excitation," Soil Dynamic and Earthquake Engineering 2004, vol. 24, pp 537-550.
22 Psarropoulos, P.N., Klonaris, and Gazetas, G. "Seismic earth pressures on rigid and flexible retaining walls," Soil Dynamic and Earthquake Engineering 2005, vol. 25, pp 795-809.
23 ADINA software manuals, 2000.

11/10/2012